第 36 卷第 5 期 无 机 化 学 学 报 Vol.36 No.5
2020 年 5 月 CHINESE JOURNAL OF INORGANIC CHEMISTRY 958-968

助剂对 Ni-Al 合金和 Raney-Ni 催化剂结构及 1,4-丁烯二醇加氢性能的影响

郜宪龙 莫文龙* 马凤云 樊 星
(煤炭洁净转化与化工过程新疆维吾尔自治区重点实验室,新疆大学化学化工学院,乌鲁木齐 830046)

摘要:采用等体积浸渍法将助剂(MgO、CuO、Co_2O_3)引入商品 Ni-Al 合金粉,经 10%(*w*/*w*)NaOH 溶液浸取制备 Raney-Ni 催化剂。通过能量色散 X 射线(EDX)、X 射线衍射(XRD)、N_2 吸附-脱附测试、透射电镜(TEM)、NH_3 程序升温脱附(NH_3-TPD)、X 射线光电子能谱(XPS)等方法表征和评价实验,考察了金属助剂对 Ni-Al 合金粉及 Raney-Ni 催化剂元素组成、晶相结构、孔结构特征、表面形貌、表面酸碱性的影响。表征分析显示,不同助剂催化剂的元素含量、比表面积及表面形貌均表现出明显的差异。其中,添加助剂 Cu 的催化剂表面检测到较多的活性组分 Ni,接近 90%(*w*/*w*),该催化剂平均孔径最小(3.87 nm)、活性组分 Ni 颗粒分散性好。评价结果表明,该催化剂具有较佳的加氢性能,其 1,4-丁烯二醇(BED)转化率为 100%,1,4-丁二醇(BDO)选择性和收率分别为 59.62%和 59.62%,这与该催化剂较大的活性组分 Ni 负载量、酸强度和适中的酸量及存在的 Cu 对 Ni 分散性的提高进一步防止了 Ni 的严重烧结(即"限域效应")等有较大关联。

关键词:Raney-Ni 催化剂;1,4-丁烯二醇;1,4-丁二醇;助剂;加氢
中图分类号:O643.32 **文献标识码**:A **文章编号**:1001-4861(2020)05-0958-11
DOI:10.11862/CJIC.2020.102

Effect of Promoter on the Ni-Al Alloy & the Corresponding Raney-Ni Catalyst and Hydrogenation Performance of 1,4-Butylenediol

GAO Xian-Long MO Wen-Long* MA Feng-Yun FAN Xing
(*Key Laboratory of Coal Clean Conversion & Chemical Engineering Process (Xinjiang Uyghur Autonomous Region), College of Chemistry and Chemical Engineering, Xinjiang University, Urumqi* 830046, *China*)

Abstract: Three promoters (MgO, CuO, Co_2O_3) were introduced individually into the commercial Ni-Al alloy powder by impregnation method, and the modified alloys were leached by 10%(*w*/*w*) NaOH solution to prepare Raney-Ni catalysts. Effect of promoter on the elemental composition, crystal structure, pore structure, surface morphology and surface acidity of the Ni-Al alloy and the corresponding Raney-Ni catalyst was investigated by energy dispersive X-ray (EDX), X-ray diffraction (XRD), N_2 adsorption-desorption, transmission electron microscope (TEM), NH_3 temperature programmed desorption (NH_3-TPD) and X-ray photoelectron spectroscopy (XPS) methods. Results showed that the element content, specific surface area and surface morphology of the catalyst modified by different promoter proposed significant difference. Large amount of Ni- the active component on the Cu-modified catalyst was detected with the content of about 90% (*w*/*w*), showing excellent dispersion, and the catalyst presented small average pore size (3.87 nm). Evaluation results showed that the catalyst displayed well hydrogenation performance, with 1,4-butenediol (BED) conversion of 100%, both 1,4-butanediol (BDO) selectivity and yield of 59.62%, which was related to the high Ni content, the moderate amount of acid sites and the small Cu crystal for improving Ni dispersion without serious sintering by the "confinement effect".

Keywords: Raney-Ni catalyst; 1,4-butenediol; 1,4-butanediol; promoter; hydrogenation

收稿日期:2019-12-19。收修改稿日期:2020-03-13。
新疆维吾尔自治区重点研发计划项目(No.2017B02012)和新疆大学自然科学基金项目(No.BS160221)资助。
*通信联系人。E-mail:mowenlong@xju.edu.cn

0 Introduction

Selective hydrogenation of C=C to C-C is of importance to produce valuable or fine chemicals. 1,4-butanediol (BDO) is one of the widely used chemical raw materials, which is used to produce polybutylene terephthalate (PBT), tetrahydrofuran (THF), γ-butyllactone (GBL), polyurethane thermoplastic elastomer and fiber[1-3]. Demanding of BDO would continue to grow because of the widely used of it and its derivatives. High pressure hydrogenation process, which is easy to cause safety problems, has long been adopted to produce BDO in industry. While it has become the focus of researchers to explore the hydrogenation process under low pressure by improving catalyst component and structure[4]. Hydrogenation process of 1,4-butenediol (BED) is commonly accompanied with side reactions, including double bond migration, hydrogenolysis, isomerization, to form 4-hydroxybutanal (HALD), THF, 1-ene-3-octanol ($C_8H_{16}O$, EO), 2-hydroxytetrahydrofuran (HTHF) and 2-(4-hydroxybutoxy)-tetrahydrofuran (HBOTHF). Therefore, well tuneable hydrogenation performance of BED to BDO is crucial for industrial application. And the common used catalyst for BDO production from BED is Raney-Ni.

Raney-Ni catalyst has long been widely used since 1925. Compared with precious metal catalysts, Raney-Ni was thought as a relatively inexpensive and cost-effective catalyst[5]. It has been developed into a class of widely used catalysts in the production of sorbitol, methyl-ethanone, aliphatic amine, hydrogen peroxide, spices, hexylenediamine and other products[6-8]. In addition, Raney-Ni catalyst has the advantages of simple preparation, well heat conduction, high activity and strong stability[9].

Lei et al.[10] found that the activity of Raney-Ni catalyst prepared by fast setting technology was 5 times higher than the catalyst by traditional methods. DuPont reported that alkali leaching of 35%~66%(*w*/*w*)Ni/40%~65%(*w*/*w*) alloy was used to obtain skeleton Raney-Ni catalyst with a certain ratio of Ni to Al, which showed excellent hydrogenation performance. US patent[11] showed that 3%~25%(*w*/*w*) Cu was introduced into Raney-Ni catalyst to prepare Cu-modified Raney-Ni catalyst. The catalyst was applied to the hydrogenation of BED. The activity and selectivity of the catalyst were determined under the temperature of 20~140 ℃ and hydrogen pressure of 0~2 MPa. In addition, Raney-Ni-Mo catalyst were developed, which were evaluated by hydrogenation of 1,4-butynediol (BYD) to produce BDO [12]. Therefore, the modified Raney-Ni catalyst could improve the distribution of active components, crystal structure, pore structure, surface morphology and surface acidity of the catalyst.

Generally, catalyst hydrogenation performance is related to its mechanical strength, carbon deposition resistance[13], nickel content[14], promoter type and amount[15-16], preparation method[17] and so on. Raney-Ni presented well performance in hydrogenation, dehydrogenation, dehalogenation and other chemical conversions due to its well heat conduction, high catalytic activity and strong stability. In the traditional BED hydrogenation process, noble mental (Ru, Pt, Pd, *etc*.) catalysts exhibited high catalytic activity. However, noble metals are scarce and expensive, which limit the large-scale application in industry. In order to meet the industrial demand, it is necessary to develop economical catalyst, such as Raney-Ni. It is reported that skeleton structure catalysts (catalyst prepared from an alloy) can display well catalytic properties (*e.g.* activity, selectivity and stability) during the hydrogenation process, which are superior to nickel-based catalysts. Xu et al.[18] investigated the effect of Raney-Ni-X (Fe, Mo, Cr) catalyst on the hydrogenation performance of glucose. Results showed that the Raney-Ni catalysts modified by Fe, Mo and Cr exhibited excellent performance. And Raney-Ni-Mo performed better stability and activity than others. On the one hand, the promoter of Mo could increase the specific surface area of Raney-Ni catalyst from 77 to 83 $m^2 \cdot g^{-1}$. On the other hand, the addition of Mo could prevent Ni from being oxidized. Wang et al.[19-20] investigated the effect of different additive on the hydrodeoxygenation performance of Ni-based catalysts. Results showed that Fe could significantly increase the dispersion of active component Ni and improve the

activity. Effect of Mo on the hydrogenation performance of Ni-based catalyst was also observed. The results proposed that the metal-Mo not only improved the dispersion of Ni, but also enhanced the interaction force between Mo and the carrier. In summary, the additive could change catalyst structure and affect its performance[21-23]. In addition, the application of Mg, Cu and Co modified catalysts was beneficial to hydrogenation.

In this paper, the modified Ni-Al alloy powder by metal promoter was prepared by impregnation method, and leached by NaOH solution (10%(*w*/*w*)) to remove Al to obtain Raney-Ni catalyst. And the catalysts were characterized by energy dispersive X-ray (EDX), X-ray diffraction (XRD), N_2 adsorption-desorption, transmission electron microscope (TEM), NH_3 temperature programmed desorption (NH_3-TPD) and X-ray photoelectron spectroscopy (XPS) methods. Effect of Mg, Cu and Co on the structure of Ni-Al alloy and the corresponding Raney-Ni catalyst and its hydrogenation performance of BED were investigated.

1 Experimental

1.1 Preparation of catalyst

The modified Ni-Al alloy powder was prepared by impregnation method. Commercial Ni-Al powder (100~120 mesh) was added to nitrate solution of different metal. The above mixture was put in ultrasonic machine for 0.5 h, stirred for 0.5 h, impregnated for 24 h, dried at 110 ℃ for 4 h and calcinated at 450 ℃ for 3 h in a muffle furnace, and the modified Ni-Al alloy powder could be obtained. The prepared alloys were labeled as RN_{Mg}, RN_{Cu} and RN_{Co} according to the added promoter. The commercial Ni-Al alloy powder was marked as RN. Prepared Ni-Al alloys were leached by 10%(*w*/*w*) NaOH solution at 80 ℃ for 90 min, and the mixture was washed with anhydrous ethanol for several times, then Raney-Ni catalysts were obtained. The synthesized catalysts were correspondingly labeled as CRN, CRN_{Mg}, CRN_{Cu} and CRN_{Co}.

1.2 Characterization of catalyst

X-ray diffraction (XRD) analysis was carried out on an X-ray diffraction (Rigaku D/Max-2500, Japan) using nickel filtered Cu $K\alpha$ (λ=0.154 06 nm) radiation. The scan rate, diffraction range, tube voltage and tube current were 8°·min^{-1}, from 5° to 85°, 40 kV and 100 mA, respectively. N_2 adsorption-desorption profiles at −196 ℃ were obtained by a Quantachrome Automated Gas Sorption apparatus (Micromeritics ASAP 2020). Energy dispersive X-ray (EDX) analysis was carried out on LEO 1530VP spectrometer from Germany with accelerating voltage of 20 kV, working distance of 15 mm and acquisition time of 120 s. Transmission electron microscopy (TEM) micrograph was obtained using a JEOL JEM-2100 election microscope operating at 200 kV. Acidic properties of the catalysts were measured via a temperature-programmed desorption of ammonia (NH_3-TPD) using a Quantachrome Chemisorb instrument. The chemical states of the catalysts were analyzed by X-ray photoelectron spectroscopy (XPS) using a Thermo Scientific instrument and Kα surface analysis.

1.3 Catalytic performance

BED hydrogenation was conducted in a 50 mL high-pressure reactor (Dalian Tongda reactor factory, CJF-605, China), and the liquid products were analyzed using a gas chromatography (GC-2014C, Shimadzu instrument Co. Ltd., Japan). Fig.1 shows the schematic setup of hydrogenation and product analysis system. BED hydrogenation was carried out at 120 ℃ under 5.0 MPa for 3 h, with stirring rate of 400 r·min^{-1} and catalyst addition of 0.4 g. The feedstock was 30 mL aqueous solution containing 35%(*w*/*w*) BED.

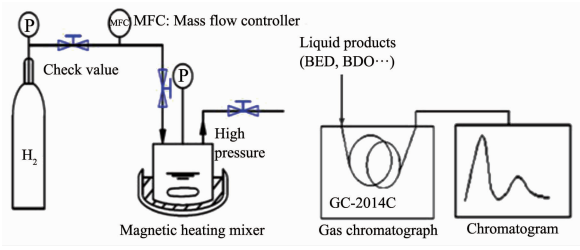

Fig.1 Scheme profile of the evaluation device for BED hydrogenation

BDO, BED, butyric anhydride (BA) and THF were the main substances in the catalytic hydrogenation product of BED, which were detected by SH-Rtx-Wax

capillary column. The performance of hydrogenation catalyst was evaluated by BED conversion (X), BDO selectivity (S) and yield (Y), which can be calculated by equation (**1**), (**2**) and (**3**), respectively.

Performance of the catalyst:

$$X=1-C_3/(C_1+C_2+C_3+C_4)\times 100\% \quad (1)$$

$$S=C_2/(C_1+C_2+C_4)\times 100\% \quad (2)$$

$$Y=X\times S\times 100\% \quad (3)$$

where C_i represent the molar percentage of the corresponding substance; i=1, 2, 3 and 4 representing components BED, BDO, BA and THF, respectively.

2 Results and discussion

2.1 Alloy powder characterization

2.1.1 XRD analysis

Fig.2 shows the XRD patterns of alloy powders modified with different additives. All the samples were composed of two crystals (Ni_2Al_3 and $NiAl_3$). The diffraction peak positions of Ni_2Al_3 was located at 2θ= 18.0°, 25.5°, 31.4°, 45.2°, 48.8°, 55.9°, 59.4° and 69.5°. The peak positions of $NiAl_3$ was detected at 2θ=19.2°, 23.0°, 29.7° , 37.1°, 38.8°, 41.4°, 41.9°, 43.7°, 44.9°, 46.4°, 47.3°, 62.7° and 65.5°. The diffraction peak positions of $NiAl_3$ and Ni_2Al_3 were the same for each modified alloy, while the intensity and the half-peak width were quite different. The intensity

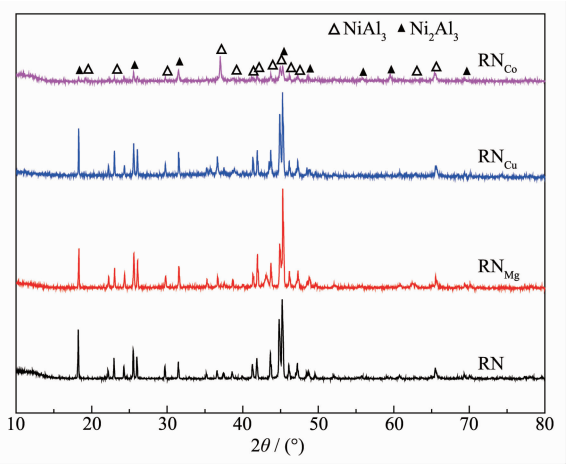

Fig.2　XRD patterns of the alloys modified with different promoters

of $NiAl_3$ and Ni_2Al_3 was significantly weakened with the addition of Co, and the peak shape was more dispersed, resulting in the increase of half-peak width.

The diffraction peaks of Cu, Mg and Co were not detected by XRD characterization in the modified Ni-Al alloys, indicating that the promoter of Cu, Mg and Co might be highly dispersed on the Ni-Al surface without the formation of promoter crystal.

2.1.2 TEM

Fig.3 gives the TEM photograph of the Ni-Al alloy. The surface morphology of all the samples was in the form of sheet-like particle. It could be clearly

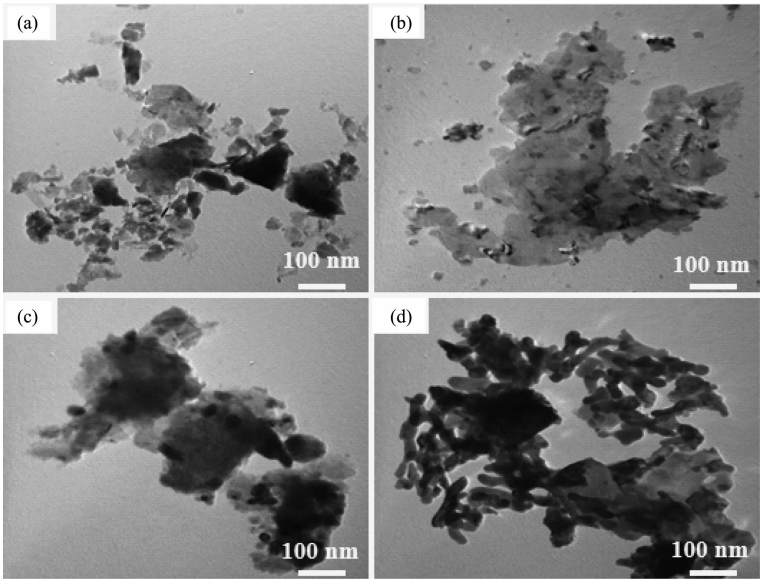

(a) RN; (b) RN_{Mg}; (c) RN_{Cu}; (d) RN_{Co}

Fig.3　TEM images of the alloys

observed that there was many pieces for the RN_{Mg} sample, and the pieces was more concentrated and uniform than the other catalysts. Therefore, the introduction of metal could significantly make the morphology of the Ni-Al alloy powder more regular.

2.2 Catalyst characterization

2.2.1 EDX and EDX-mapping

EDX analysis was carried out for the prepared catalysts, and the results are given in Table 1. The elements of Ni, Al, Mg, Cu and Co in all samples were found by EDX test. It could be seen from Table 1 that the CRN and CRN_{Cu} presented a high Ni/Al molar ratio (n_{Ni}/n_{Al}), and the n_{Ni}/n_{Al} for the two samples were 3.93, indicating that the Ni content of the sample was high with more active sites. The CRN sample showed a high Ni content of 89.53% (*w*/*w*), which was 187% higher than that of RN (48%(*w*/*w*)), demonstrating that a large amount of Al was washed away by NaOH solution during the leaching process (① $Al^{3+}+4OH^- \rightarrow [Al(OH)_4]^-$, ② $[Al(OH)_4]^- \rightarrow Al(OH)_3+OH^-$, the Al element would be transformed into hydrated alumina and precipitated in the form of aluminum hydroxide). And there is a part of Al element retained in the catalyst. The skeleton structure of the catalyst would be severely collapsed once the Al was completely leached, which might cause particle agglomeration and reduce the activity of the catalyst. Therefore, the residual amount of Al element had a significant effect on maintaining the activity of the catalyst[24-25].

The relative content of the three promoters was between 1.35% and 1.75%, while the corresponding M_yO_x content of each catalyst was calculated to be about 2.3% (*w*/*w*). More active component-Ni was detected in the sample CRN_{Cu}, about 90%(*w*/*w*), higher than CRN_{Mg} and CRN_{Co} (about 80%(*w*/*w*)), indicating that there were more active sites on the surface of the CRN_{Cu} catalyst. According to the principle of EDX method, the content of Ni element on the surface of the catalyst can only be measured at nanometer thickness. With the addition of Co, Cu and Mg, the distribution of the active component Ni on the catalyst was changed, resulting in a great difference in the content of Ni measured.

D_{Ni} calculated by Scherrer formula at 2θ angles of Ni(111) was the Ni grain size, as shown in Table 1. To observe the dispersion of each element in the catalyst, the EDX-mapping test was performed to verify the distribution of each element on the Raney-Ni catalyst surface. Fig.4 shows the EDX-mapping diagrams of all the catalysts. It could be seen from the mapping diagrams that the Mg, Cu and Co elements were distributed on the surface of each catalyst, indicating that the Mg, Cu and Co elements in the prepared catalyst could be uniformly distributed by impregnation method. The Al element distribution on the surface of the CRN_{Cu} sample was relatively sparse, which was consistent with the small Al content of 10.29%(*w*/*w*).

2.2.2 XRD analysis

Fig.5 gives the XRD patterns of Raney-Ni catalysts. The characteristic diffraction peaks of Ni were detected in each sample at 2θ=43.9°, 51.5° and 77.1°, corresponding to Ni(111), Ni(200) and Ni(220), respectively[26]. The diffraction peaks of the promoters of Mg and Co were not detected in Fig.5. The reason might be that the two promoters could not form crystal or were dispersed in amorphous state on the inner and outer surfaces of the catalyst[27]. While the CRN_{Cu} catalyst presented the characteristic peaks of Cu at 2θ=43.3°, 50.4° and 74.1°. This might be derived from the reason that a large amount of H_2 were produced during the leaching process of Ni-Al alloy powder,

Table 1 Element content, Ni crystal size of the catalysts

Sample	w_{Ni} / %	w_{Al} / %	w_{Mg} / %	w_{Cu} / %	w_{Co} / %	n_{Ni}/n_{Al}	D_{Ni}^* / nm
CRN	89.53	10.47	—	—	—	3.93	0.232
CRN_{Mg}	79.34	19.32	1.35	—	—	1.89	0.254
CRN_{Cu}	87.97	10.29	—	1.74	—	3.93	0.280
CRN_{Co}	79.56	18.69	—	—	1.75	1.96	0.297

*Calculated by Scherrer formula at 2θ angles of Ni (111)

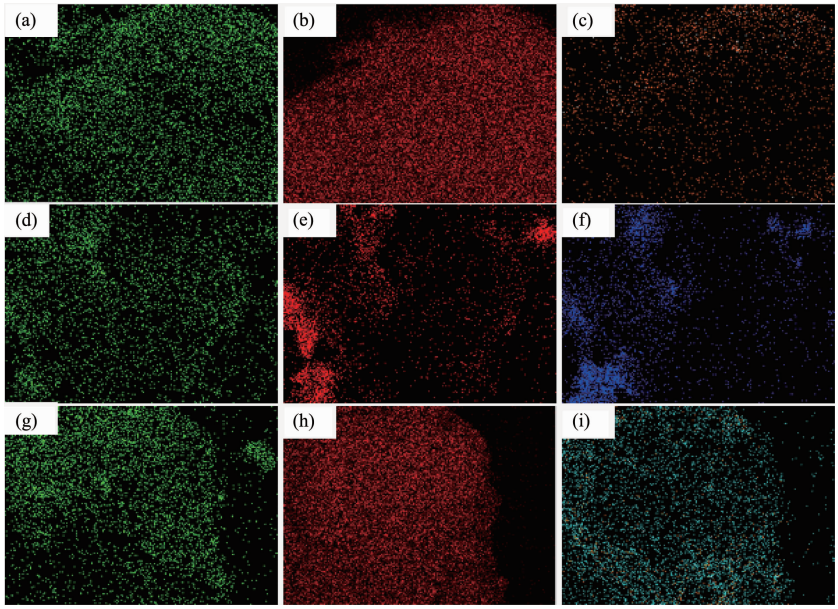

(a) CRN_{Mg}-Al; (b) CRN_{Mg}-Ni; (c) CRN_{Mg}-Mg; (d) CRN_{Cu}-Al; (e) CRN_{Cu}-Ni; (f) CRN_{Cu}-Cu; (g) CRN_{Co}-Al; (h) CRN_{Co}-Ni; (i) CRN_{Co}-Co

Fig.4　EDX-mapping photos of the catalysts

and the H_2 was to act as a reducing agent to reduce CuO to Cu metal [28]. And the small Cu crystal was beneficial for improving Ni dispersion without serious sintering by the "confinement effect"[29-30]. In addition, the intensity of the diffraction peaks of Ni increased with the introduction of Mg, Cu and Co metal, indicating that the crystal size of Ni increased (Table 1).

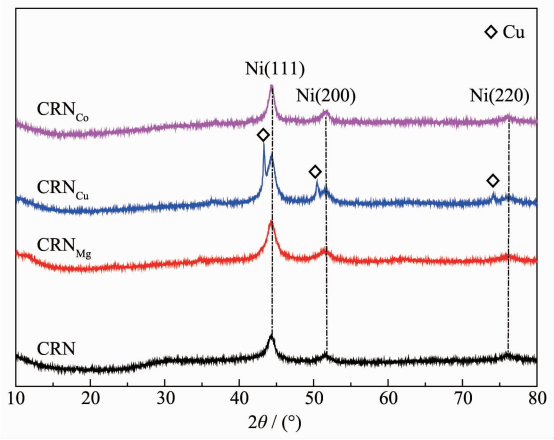

Fig.5　XRD patterns of the catalysts

2.2.2　N_2 adsorption-desorption analysis

The N_2 adsorption-desorption results of the prepared catalysts are shown in Fig.7. According to the International Union of Pure and Applied Chemistry (IUPAC) classification, it could be advised that there was H3 hysteresis loops for all the catalysts, and the isothermal adsorption lines were ascribed to type Ⅲ, indicating that the adsorption heat is smaller than the liquefaction heat[31].

Fig.6(a) shows the N_2 adsorption-desorption isotherms of Raney-Ni catalysts. CRN_{Mg} presented a large hysteresis loop, while the loop of CRN_{Co} was small. The area of the loop of CRN_{Mg} catalyst was larger than that of CRN catalyst, while the loops area of CRN_{Mg} and CRN_{Cu} catalysts decreased.

Fig.6(b) gives the BJH (Barrett-Joyner-Halenda) pore size distributions of the catalysts. All the samples presented the pore size of 10~100 nm, and the most probable pore diameter of each sample was distributed at 12 and 50 nm, demonstrating that the four samples were ascribed to mesoporous-mesoporous multi-level material. The peak shape of each sample was nearly the same, indicating that the addition of promoter didnt obviously change the pore structure of the CRN sample.

According to N_2 adsorption-desorption isotherms, the specific surface area of each sample was calculated by BET (Brunauer-Emmett-Teller) equation, and the pore volume and average pore diameter were calculated by BJH equation, as shown in Table 2. The specific surface area of all the samples was between

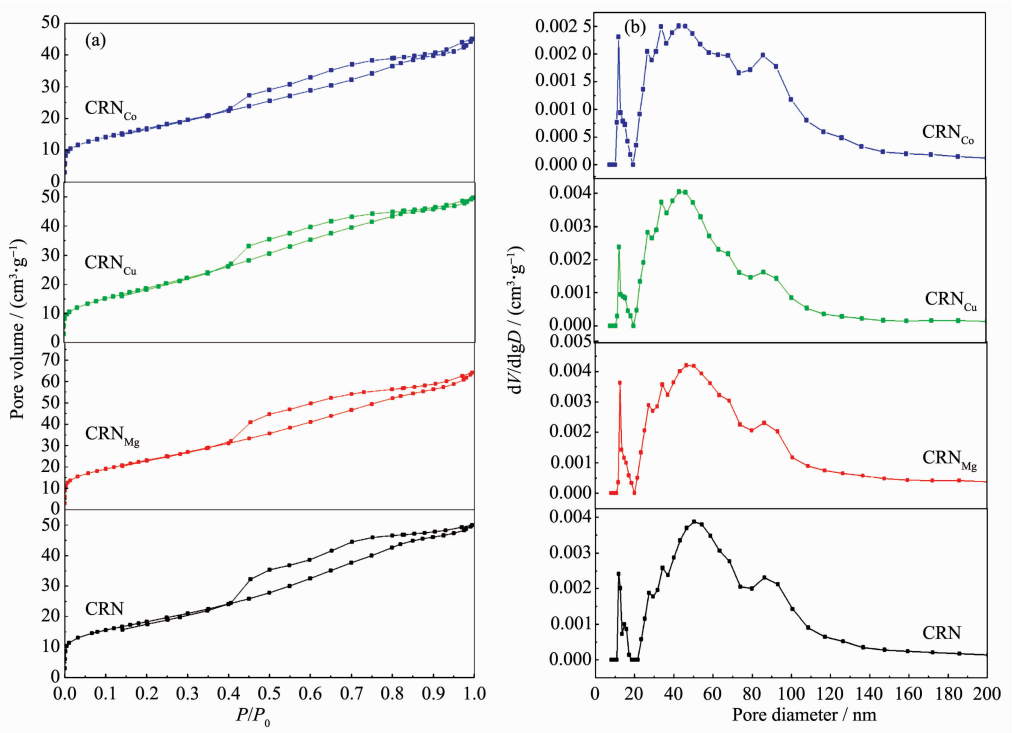

Fig.6 N_2 adsorption-desorption isotherms (a) and pore size distribution curves (b) of the catalysts

Table 2 Specific surface area, pore volume, average pore diameter of the catalysts

Samples	Specific surface area[a] / (m^2·g^{-1})	Pore volume[b] / (cm^3·g^{-1})	Average pore diameter[c] / nm
CRN	66	0.071	4.29
CRN$_{Mg}$	85	0.092	4.32
CRN$_{Cu}$	71	0.072	3.87
CRN$_{Co}$	61	0.065	4.44

[a]Calculated by BET equation; [b]BJH desorption average pore diameter; [c]BJH desorption pore volume

60 and 85 m^2·g^{-1}, pore volume of 0.05~0.1 cm^3·g^{-1}, average pore diameter of 3~5 nm. And the CRN$_{Cu}$ catalyst presented small average pore diameter of 3.87 nm, specific surface area of 71 m^2·g^{-1} and pore volume of 0.072 cm^3·g^{-1}.

2.2.6 NH_3-TPD

Fig.7 gives the NH_3-TPD diagram of the catalysts. Only one NH_3 desorption peak was detected in CRN, and two distinct NH_3 desorption peaks appeared in other catalysts. The CRN, CRN$_{Co}$ and CRN$_{Mg}$ samples showed the first peak at around 325 ℃, while the peak of the CRN$_{Cu}$ catalyst was around 385 ℃. The CRN$_{Mg}$ catalyst showed the second NH_3 desorption peak at around 445 ℃, CRN$_{Cu}$ around 430 ℃, and CRN$_{Co}$ dropped to about 410 ℃, indicating that there are mainly two kinds of acid center on the surface of Raney-Ni catalyst. The former was located in the temperature of 320~390 ℃, corresponding to the weak acid center[32]. The latter was located in the temperature of 390~450 ℃, corresponding to the medium acid center[33]. The temperature of the medium acid peaks

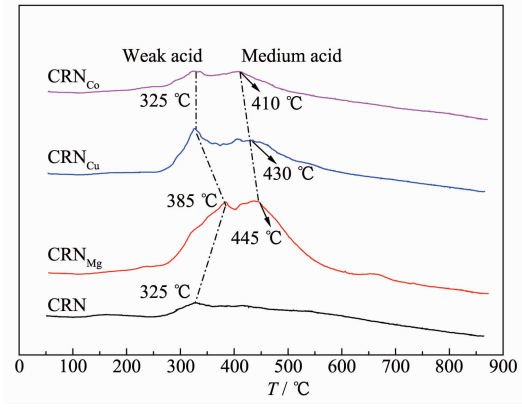

Fig.7 NH_3-TPD results of the catalysts

presented the following order: $T_{CRN_{Mg}}>T_{CRN_{Co}}>T_{CRN_{Cu}}$. The peak temperature of the weak and medium acids were large (385 and 445 ℃) for the CRN_{Mg} catalyst. In addition, with the addition of Co, Cu and Mg promoters, the corresponding peaks area showed an increasing tendency, indicating that the number of acid centers increased.

The peak area of weak acid and medium acid was further fitted by Peakfit software, and the peak area percentage was estimated, as shown in Table 3. The percentage of peak area of the modified samples was larger than CRN, with the medium acid peak area of CRN_{Mg} catalyst of 52%. In addition, The addition of alkaline additive-Mg promoted the absorption of NH_3 on the surface of Raney-Ni catalyst, resulting in strong acidity of the catalyst.

Table 3　Peak area proportion of weak acid and medium acid

Sample	Peak area proportion of the weak acid / %	Peak area proportion of the medium acid / %
CRN	100	0
CRN_{Mg}	48	52
CRN_{Cu}	54	46
CRN_{Co}	50	50

2.2.7　XPS

To investigate the valence state of the catalysts, all the samples were characterized by XPS test, as shown in Fig.8. It could be found that the intensity of Ni2*p* peak at 856.7 eV was different for each catalyst, which might be derived from the dispersion effect caused by the addition of different promoter (Mg, Cu, Co). In addition, the peaks of promoters were detected at 1 305.2, 951.5 and 780.5 eV, respectively, which could be ascribed to Mg2*p*, Cu2*p*, and Co2*p* (Fig.8). Literature showed that the peaks at 932.5 and 952.5 eV were assigned to the Cu^0 / Cu^+ peak and the Cu^{2+} peak, respectively[34].

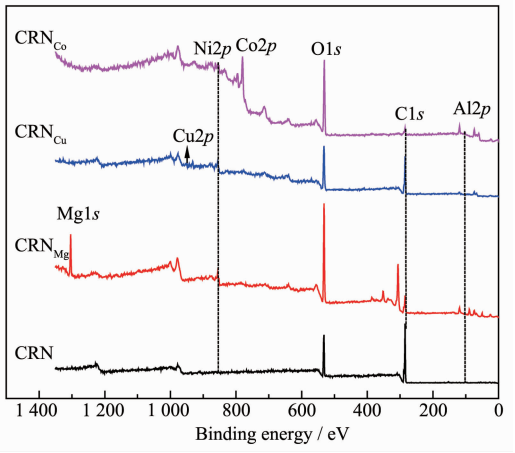

Fig.8　Total XPS spectra of the catalysts

The XPS spectra of the $Ni2p_{3/2}$ were shown in Fig.9 and Table 4. Fig.9(a) showed that the binding energy at the range of 840~890 eV were attributed to $Ni2p_{3/2}$. Two $Ni2p_{3/2}$ peaks ($Ni2p_{3/2}$-1 and $Ni2p_{3/2}$-3) in Fig.9(b) were detected in the CRN sample, one at 854.4 eV and another at 862.2 eV, and the corresponding binding energy was higher than the modified catalyst, indicating that the Ni^{2+} in the CRN catalyst was more stable. With the addition of promoter, the binding energy of $Ni2p_{3/2}$-1 and $Ni2p_{3/2}$-3 peaks was decreased, which might be attributed to the calcination process at high temperature (450 ℃). The peaks of CRN_{Cu} at 852.1, 856.0, 859.3 and 862.4 eV were attributed to the Ni^0 peak, Ni^{2+} and the corresponding satellite peaks[27], respectively. Compared with the samples without additive, the peaks of Ni^0 and Ni^{2+}

Table 4　Binding energy of $Ni2p_{3/2}$ of the catalysts

Sample	Binding energy / eV (±0.3 eV)			
	$Ni2p_{3/2}$-1	$Ni2p_{3/2}$-2	$Ni2p_{3/2}$-3	$Ni2p_{3/2}$-4
CRN	854.4	—	862.2	—
CRN_{Mg}	852.4	856.1	859.8	862.9
CRN_{Cu}	852.1	856.0	859.3	862.4
CRN_{Co}	852.6	855.6	859.6	861.8

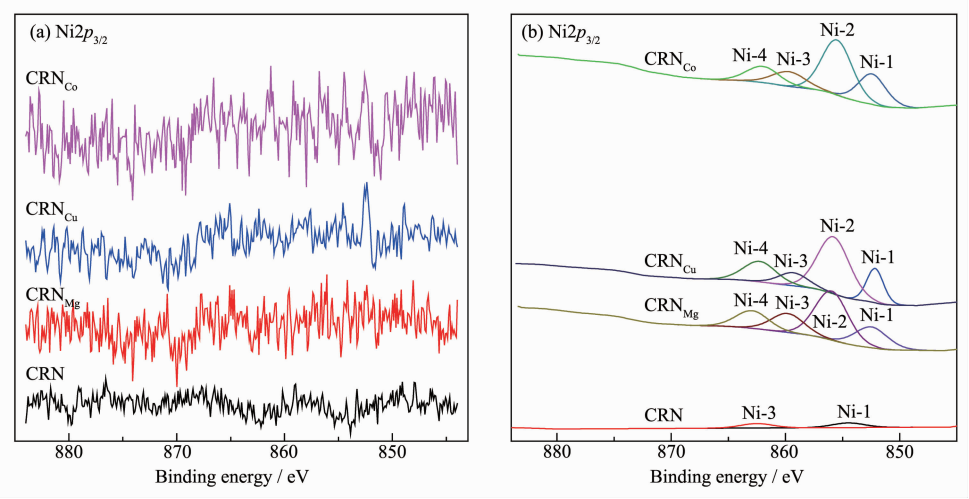

Fig.9 (a) XPS spectra of Ni2$p_{3/2}$; (b) Corresponding fitting results of Ni2$p_{3/2}$

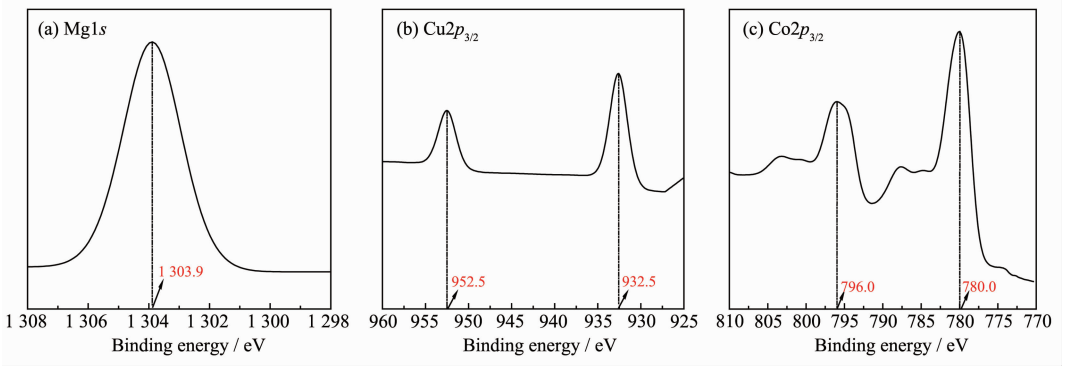

Fig.10 Fitted XPS spectra of the catalysts

accompanied by satellite peak in each sample might be derived from the addition of the additives, causing the outer electrons of Ni to the excited state, resulting in that the photoelectrons could lose kinetic energy and show higher binding energy in the spectrum. The fitted XPS spectra of the catalysts shown in Fig.10 showed that the CRN$_{Mg}$, with the addition of Mg, has only one peak, while two peaks were detected in CRN$_{Mg}$ and CRN$_{Co}$.

2.3 Catalyst activity evaluation

Fig.11 shows the evaluation results of the prepared Raney-Ni catalysts for hydrogenation performance of BED. The BED conversion of each catalyst was as high as 100%. The CRN$_{Cu}$ catalyst exhibited excellent hydrogenation selectivity, with both BDO selectivity and yield of 59.62%. According to catalyst characterizations, the reason for the better performance of the CRN$_{Cu}$ sample might be related to the following factors, such as the high n_{Ni}/n_{Al}, the small average pore diameter (3.87 nm), the moderate number of acid sites and the small Cu crystal for improving Ni dispersion without serious sintering by the "confine-ment effect". Combined with the XRD analysis, it was mainly attributed to the interaction between Ni and Cu particles, which could effectively stabilize the small

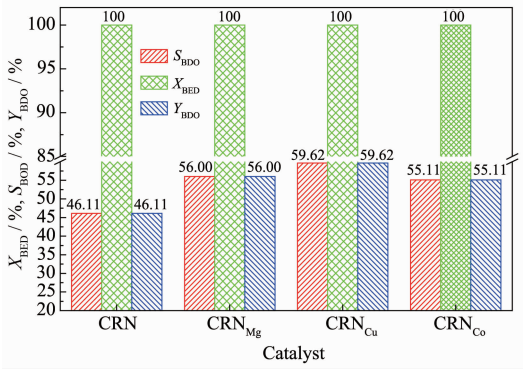

5.0 MPa (pure H_2), 393 K, 0.5 g catalyst, 30 mL BED solution (35%(w/w) in water)

Fig.11 Conversion of BED, and selectivity and yield of BDO for the catalysts

Ni particle, improving the hydrogenation activity of the catalyst. In this work, the surface acidity, the n_{Ni}/n_{Al} and the average pore diameter are the most important factors.

Fig.12 shows the selectivity distribution of hydrogenation products. The selectivity of BDO, HALD, THF, EO and others species, such as HTHF, HBOTHF, were compared. Each sample had a well selectivity for BDO. It could also be seen from Fig.12 that the selectivity of THF was high of 20% next to BDO. And the selectivity of BDO, THF, BA and EO were followed the order of BDO>THF>BA>EO.

Based on previous reports[35-37] and current experimental results, a possible reaction pathway was proposed (Fig.13). The raw material was a mixture of *cis*-BED and *trans*-BED, of which part was hydrogenated to obtain the target product BDO. The other part was isomerized to produce 4-hydroxybutyraldehyde. In addition, THF, EO and BA were obtained by a series of chemical reactions. There were also a very small amount of HALD to produce 1-hydroxyl cyclobutyl ether by cyclization, and to form HBOTHF by condensation reaction.

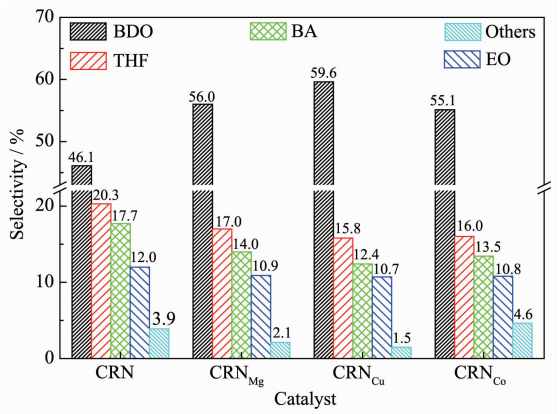

5.0 MPa (pure H_2), 393 K, 0.5 g catalyst, 30 mL BED solution (35%(*w*/*w*) in water)

Fig.12 Selectivity of products of different catalysts

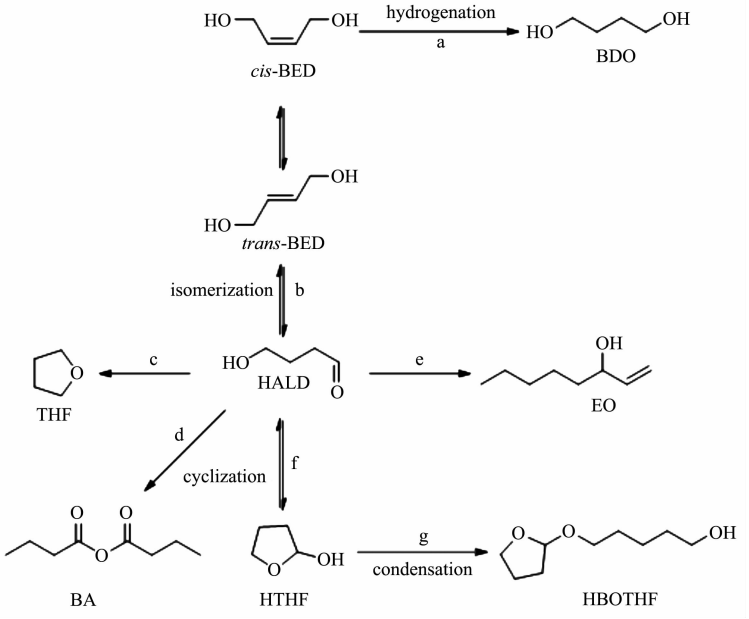

Fig.13 Proposed mechanism for hydrogenation of BED

3 Conclusions

Three promoters (MgO, CuO, Co_2O_3) were introduced individually into the commercial Ni-Al alloy powder by impregnation method, and the modified alloys were leached by 10% (*w*/*w*) NaOH solution to prepare Raney-Ni catalysts. The effect of different promoter on the structure of Raney-Ni catalyst and its hydrogenation performance of BED were investigated. It was found that the surface morphology, crystal structure, n_{Ni}/n_{Al} and surface acidity of the Ni-Al alloy and the corresponding prepared catalyst was different. Evaluation results showed that the CRN$_{Cu}$ catalyst presented well catalytic performance, with BED conversion of 100%, BDO selectivity of 59.62%, which might be related to the high n_{Ni}/n_{Al}, the

moderate amount of acid sites, the small average pore diameter (3.87 nm) and the small Cu crystal for improving Ni dispersion without serious sintering by "confinement effect".

References:

[1] Zhang Q, Zhang Y, Li H T. *Chin. J. Catal.*, **2013**,**34**:1159-1166

[2] Ildikó M, Bodor Z, Réka S, et al. *J. Biomol. Struct. Dyn.*, **2016**,**35**:1-16

[3] Minh D P, Michèle B, Pinel C, et al. *Top. Catal.*, **2010**,**53**:1270-1273

[4] Tanielyan S, Schmidt S, Marin N, et al. *Top. Catal.*, **2010**,**53**:1145-1149

[5] Kou Z N, Zhi Z N, Xu G H, et al. *Appl. Catal. A*, **2013**,**467**:196-201

[6] Amarasekara A S, Lawrence Y M, Fernandez A D, et al. *Biofuels*, **2018**,**47**:1-5

[7] Bendova D H, Weidlich D T. *Sep. Sci. Technol.*, **2017**,**53**:1-5

[8] Luo G H, Wang Y L, Sun D M, et al. *China Petroleum Processing & Petrochemical Technology*, **2017**,**19**:14-20

[9] Lei H, Song Z, Tan D L, et al. *Appl. Catal. A*, **2001**,**214**:69-76

[10]LEI Hao(雷浩). *Dalian Institute of Chemical Physics*(中国科学院大连化学物理研究所博士论文), **2003**.

[11]Hort E V, Graham D E. *US Patent*, 2967893. 1961-01-10.

[12]Codignola F, Vergini G, Gronchi P, et al. *US Patent*, 4288641. 1981-09-18.

[13]Michalska K, Kowalik P, Konkol M, et al. *Appl. Catal. A*, **2016**,**523**:54-60

[14]Peyrovi M H, Toosi M R. *React. Kinet. Catal. Lett.*, **2008**,**94**:115-119

[15]Louloudi A, Papayannakos N. *Appl. Catal. A*, **2000**,**204**:167-176

[16]Zielinski M. *Appl. Catal. A*, **2012**,**449**:15-22

[17]Savva P G, Goundani K, Vakros M, et al. *Appl. Catal. B*, **2008**,**79**:199-207

[18]XU Lei-Jin(徐雷金), KONG Ling-Niao(孔令鸟), LIU Wei(刘维), et al. *Chemical Production and Technology*(化工生产与技术), **2013**,**20**:36-41

[19]Wang X F, Wang F, Chen M Y, et al. *J. Fuel Chem. Technol.*, **2005**,**33**:612-616

[20]Huo L F, Wang X F, Hou X Y, et al. *J. Fuel Chem. Technol.*, **2007**,**35**:595-598

[21]Han X, Zhou R, Lai G H, et al. *Catal. Today*, **2004**,**93**:433-437

[22]Li Y, Zhou R X, Lai G H. *React. Kinet. Catal. Lett.*, **2006**,**88**:105-110

[23]Xue J, Cui F, Huang Z W, et al. *Chin. J. Catal.*, **2012**,**33**:1642-1649

[24]Tümer H V, Feuge R O, Cousins E R. *J. Am. Oil Chem. Soc.*, **1964**,**41**:212-214

[25]Knies S, Berweiler M, Panster P, et al. *Stud. Surf. Sci. Catal.*, **2000**,**130**:2249-2254

[26]Chai M Q, Liu X Y, Li L, et al. *Chin. J. Catal.*, **2017**,**38**:1338-1346

[27]Cai B, Zhou X C, Miao Y C, et al. *ACS Sustainable Chem. Eng.*, **2017**,**5**:1322-1331

[28]Baijot V, Mehdi D R, Rossi C, et al. *Combust. Flame*, **2017**,**180**:10-19

[29]Bian Z, Kawi S. *ChemCatChem*, **2017**,**10**:320-328

[30]Jiang B, Zhang C, Wang K Q, et al. *Appl. Therm. Eng.*, **2016**,**109**:99-108

[31]FANG Jie(方洁), LI Na(李娜), CHENG Lang(成浪), et al. *Journal of Fuel Chemistry and Technology*(燃料化学学报), **2019**,**47**:725-736

[32]Annette T, Bernd H. *Top. Catal.*, **2002**,**19**:215-223

[33]Stanciulescu M, Bulsink P, Caravaggio G, et al. *Appl. Surf. Sci.*, 2014,300:201-207

[34]Wang D, Zhang Y, Li H T. *J. Catal.*, **2012**,**33**:1229-1235

[35]Tanielyan S K, Santosh R M, Augustine R L, et al. *Org. Process Res. Dev.*, **2017**,**21**:327-335

[36]Chaudhari R V, Jaganathan R, Kolhe D S, et al. *Appl. Catal. A*, **1987**,**29**:141-159

[37]Telkar M M, Rode C V, Rane V H, et al. *Appl. Catal. A*, **2001**,**216**:13-22